Poisson's ratio of rectangular anti-chiral lattices with disorder

Artur A. Poźniak[1]
Krzysztof W. Wojciechowski[2]

[1]Institute of Physics, Poznań Universty of Technology, ul. Nieszawska 13A, 60-695 Poznań,
[2]Institute of Molecular Physics PAS, ul. M. Smoluchowskiego 17, 60-179 Poznań

17$^{\mathrm{th}}$ September 2014

AUXETICS 2014

Instead of the outline

Instead of the outline

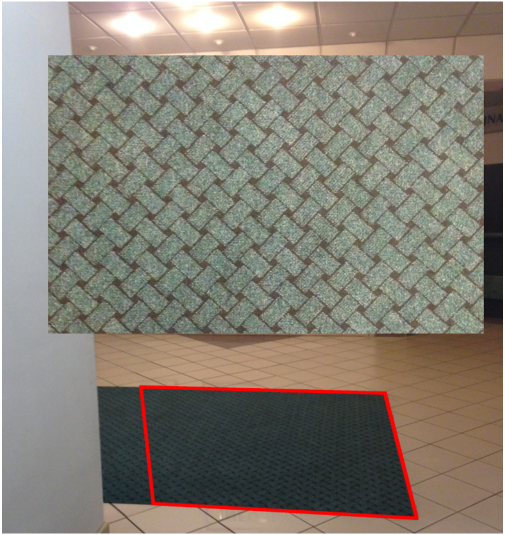

Instead of the outline

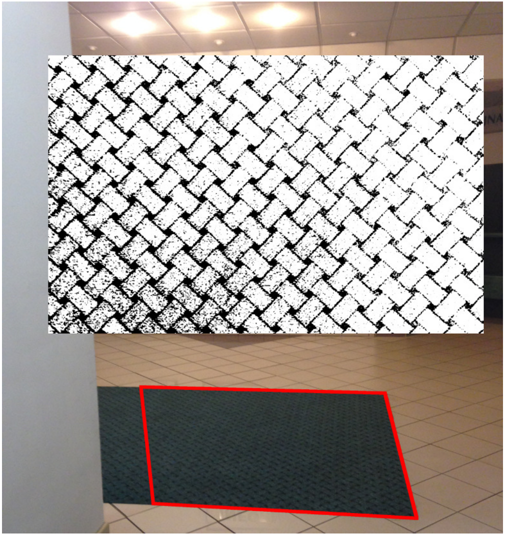

Motivation

What is an **auxetic**?

$\nu < 0$ (**N**egtative **P**oisson's **R**atio) is for mechanics what negative refractive index is for optics $n < 0$.
Auxetics are metamaterials.

Beneficial features from NPR

Resistance to shape change and indentation; crack resistance; better vibration absorption (including acoustic one); synclastic curvature, different dynamics.

Applications of NPR materials

Medicine (stents, bandages, implants), defence (energy absorption), furniture industry (better mattresses $\rightarrow$ indentation), automotive industry and sports (safety belts).

Poisson's ratio (stretching along x axis)

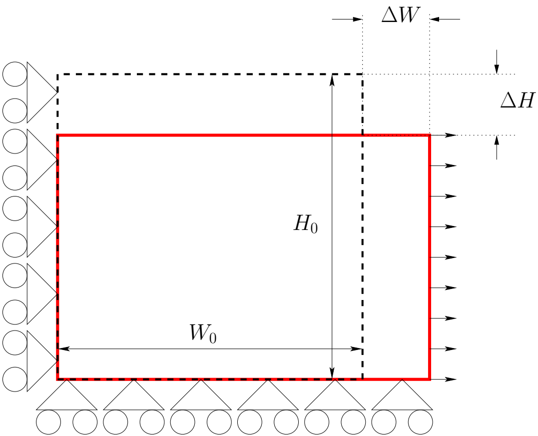

Formal definition

$$\nu_{xy} = -\frac{\epsilon_{yy}}{\epsilon_{xx}}$$

Engineering definition

$$\nu = -\frac{\dfrac{\Delta H}{H_0}}{\dfrac{\Delta W}{W_0}}$$

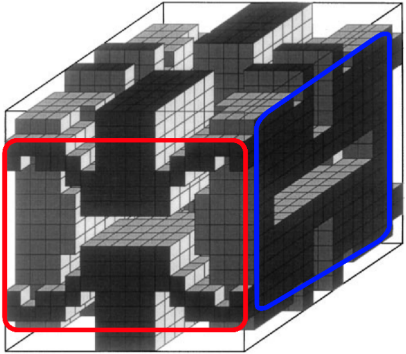

FIG. 3. Example "a": Optimal microstructure (one unit cell) for maximization of the piezoelectric charge coefficient $d_h^{(*)}$.

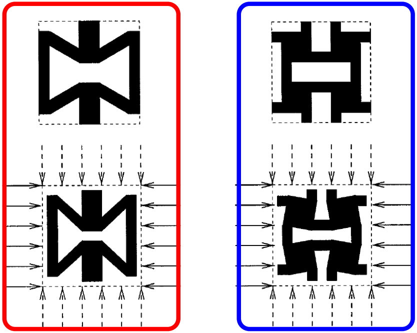

FIG. 4. Schematic representation of an equivalent two-dimensional composite that yields the (vertical) negative Poisson's ratio behavior of example "a" (Fig. 5). Left: front (1-3 plane) view, Right: side (2-3 plane) view. When the microstructures are compressed horizontally (solid arrows), they contract vertically (dashed arrows).

Source: *On the design of 1-3 piezocomposites using topology optimization*, O. Sigmund, S. Torquato, I.A. Aksay, Journal of Materials Research **13**, 4, 1040-1048 (1998)

Source: Hydrophone. (2014, February 28). In Wikipedia, The Free Encyclopedia. Retrieved 10:37, April 9, 2014

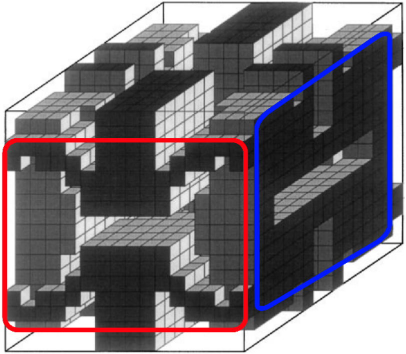

FIG. 3. Example "a": Optimal microstructure (one unit cell) for maximization of the piezoelectric charge coefficient $d_h^{(*)}$.

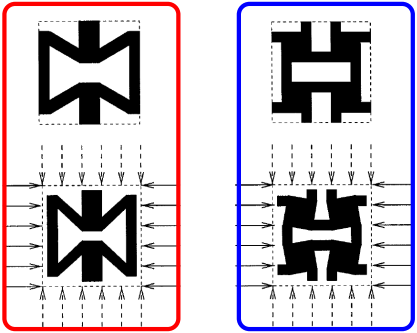

FIG. 4. Schematic representation of an equivalent two-dimensional composite that yields the (vertical) negative Poisson's ratio behavior of example "a" (Fig. 5). Left: front (1-3 plane) view, Right: side (2-3 plane) view. When the microstructures are compressed horizontally (solid arrows), they contract vertically (dashed arrows).

Source: *On the design of 1-3 piezocomposites using topology optimization*, O. Sigmund, S. Torquato, I.A. Aksay, Journal of Materials Research **13**, 4, 1040-1048 (1998)

The first article describing anti-chiral structures as NPR material. Cross sections $\rightarrow$ **different mechanisms.**

Experimental setup

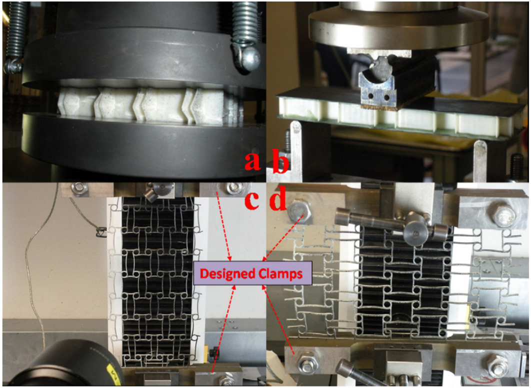

Fig. 4. Honeycomb structures experimental setup: (a) flatwise compression tests; (b) three-point bending tests; (c) and (d) tensile tests.

Source: *Elasticity of anti-tetrachiral anisotropic lattices*, Y.J. Chen et al., International Journal of Solids and Structures **50**, 996-1004 (2013)

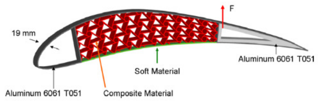

Fig. 2. Chiral core airfoil.

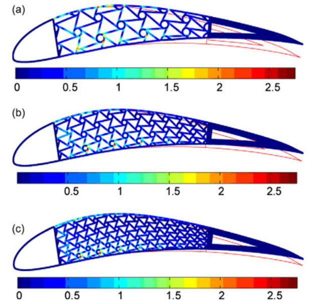

Fig. 5. Axial stress distribution ($\times 100$ MPa) at the limit of the elastic regime of the material for aluminum alloy airfoil: (a) 2-cell configuration, (b) 3 cells, and (c) 4 cells.

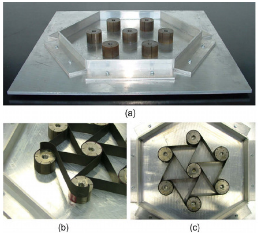

Fig. 9. Mould for component assembly (a), positioning of ligaments (b) and assembled component (c).

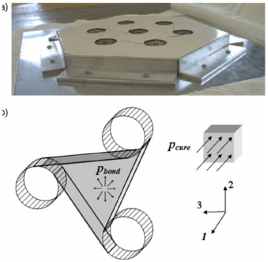

Fig. 10. Production of silicon rubber blocks (a) and application of the pressure during bonding (b).

Source: *Composite chiral structures for morphing airfoils: Numerical analyses and development of a manufacturing process*, P. Bettini et al., Compisites: Part B **41**, 2, 133-147 (2010)

Geometry

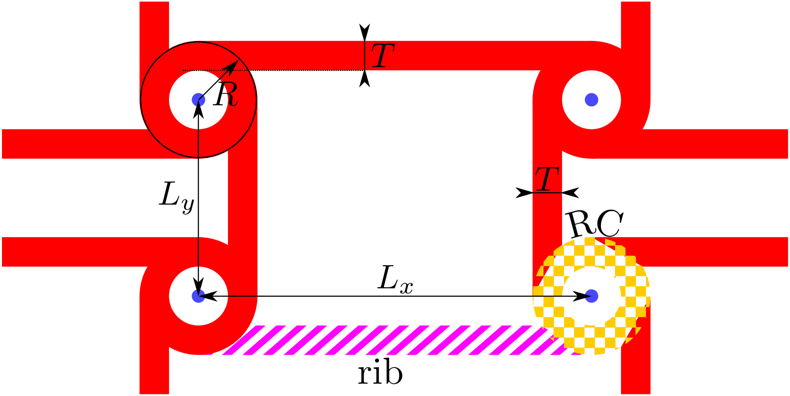

L_y is a unit length. $L_x/L_y \equiv l_y$, $T/L_y \equiv t$; taking $L_y = 1$
$l_x = L_x$ being the anisotropy parameter.

Finite Element Method

- Approximate method for solving PDEs.
- *Physical* discretization.
- Various shape functions available.
- A system of PDEs $\rightarrow$ very large system of algebraic equations.
- *Arbitrary* precision depending on t and computational resources ($).
- Variety of libraries (C$++$, Python) and proprietary software. Here Abaqus/STANDARD was employed (linear static elasticity).

Finite Element Method

- Approximate method for solving PDEs.
- *Physical* discretization.
- Various shape functions available.
- A system of PDEs $\rightarrow$ very large system of algebraic equations.
- *Arbitrary* precision depending on t and computational resources ($).
- Variety of libraries (C++, Python) and proprietary software. Here Abaqus/STANDARD was employed (linear static elasticity).

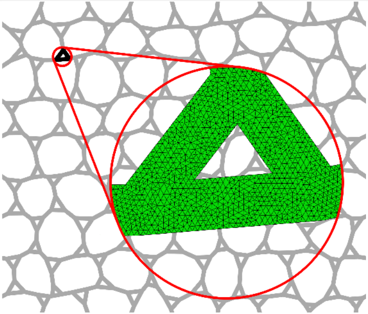

planar elements (CPS3)

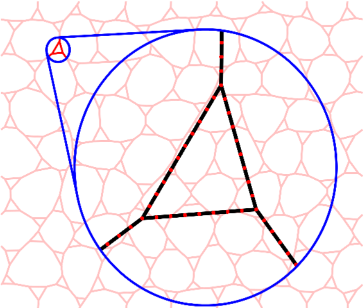

Timoshenko beam-type element(B21)

Disorder

Disorder

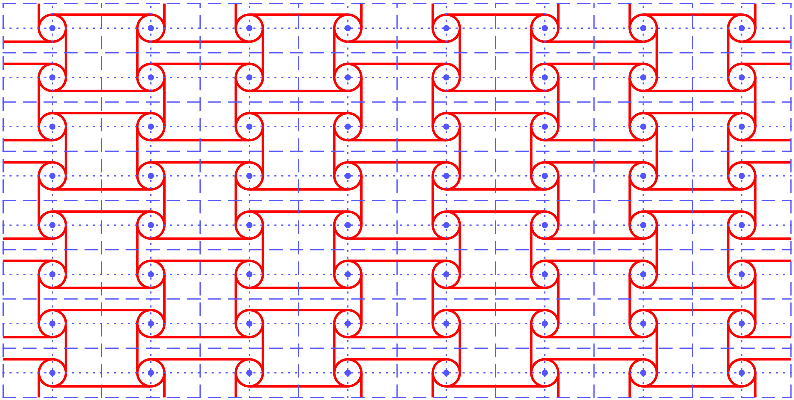

$r(=0.3) \to r + r_\delta,\ \ r_\delta \in \langle -\delta, \delta \rangle$, $\delta \le \delta_{\max}(r, L_y)$ topology remains unchanged!

Disorder

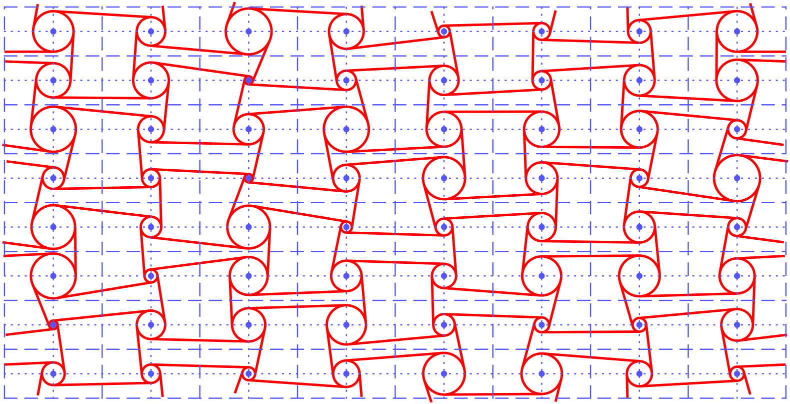

$r(=0.3) \to r + r_\delta,\ \ r_\delta \in \langle -\delta, \delta \rangle$, $\delta \leq \delta_{\max}(r, L_y)$ topology remains unchanged!

Disorder

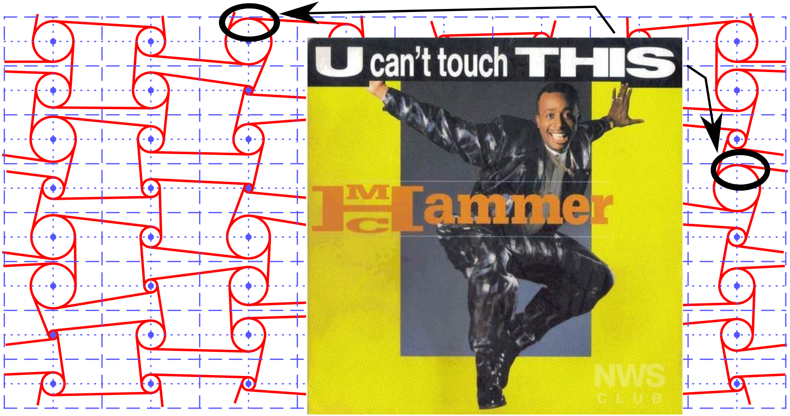

$r(=0.3) \to r + r_\delta,\ \ r_\delta \in \langle -\delta, \delta \rangle$, $\delta \leq \delta_{\max}(r, L_y)$ topology remains unchanged!

Disorder

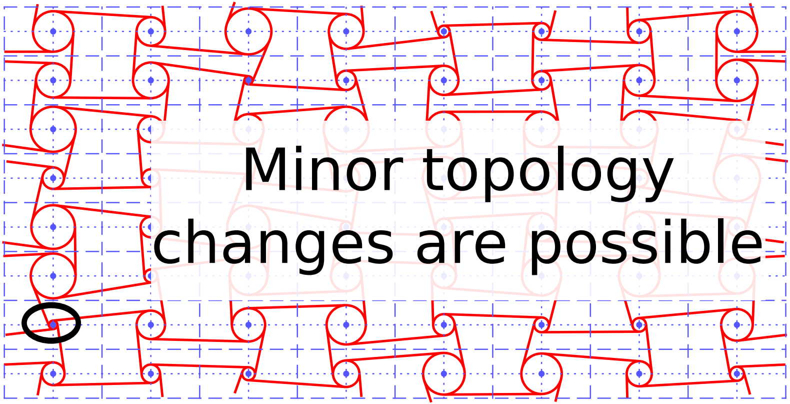

$r(=0.3) \to r + r_\delta,\ \ r_\delta \in \langle -\delta, \delta \rangle$, $\delta \leq \delta_{\max}(r, L_y)$ topology remains unchanged!

Boundary conditions

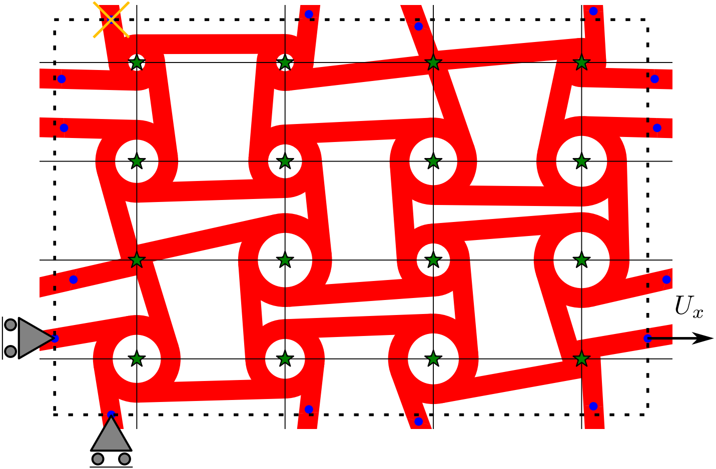

U_x is a placement-type, orange "**x**" – zero stress condition

PBC – easier for B21, CPS3 elems. require more equations – no rotational DOFs

Convergence as a function of the mesh element size CPS3

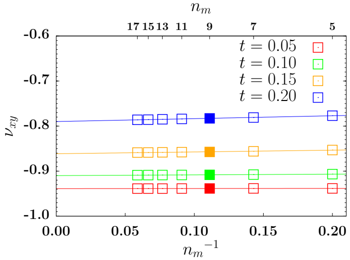

Figure: $l_x \equiv L_x/L_y = 1.0$

Filled symbol denotes mesh size chosen for further calculations corresponding to $n_x = 9$.

The figure on the right shows the case for $n_x = 7$ for clarity reasons.

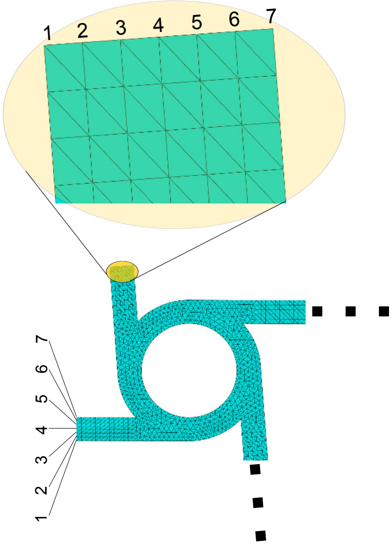

Figure: Mesh for $n_m = 7$ $(t = 0.1)$

Convergence as a function of the mesh element size B21

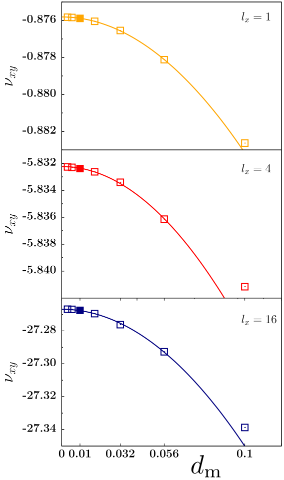

Figure: $l_x \equiv L_x/L_y = 1.0$

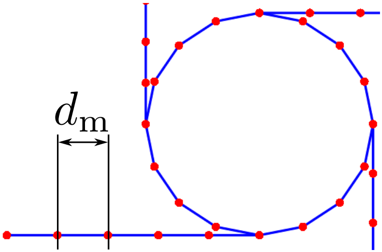

Figure: Mesh for $d_m = 0.01$ $(t = 0.1)$

Filled symbol denotes mesh size chosen for further calculations corresponding to $d_m = 0.01$.

Convergence as a function of the size of the sample

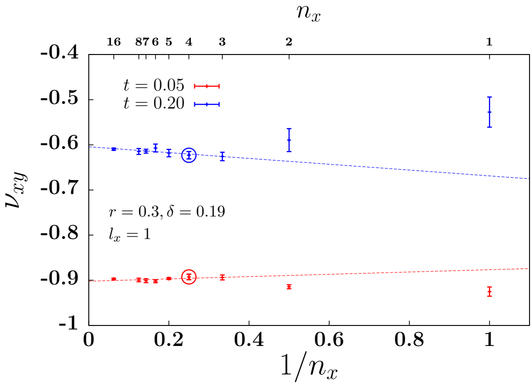

Figure: Averaged ν_{xy} for samples of size 1×1 to 16×16 of elementary units. The anisotropy parameter $l_x = 1$, $r = 0.3$ with $\delta = 0.19$ (almost maximal possible disorder). 5 samples for each average

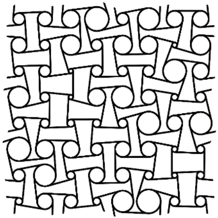

(a) $n_x = 4$

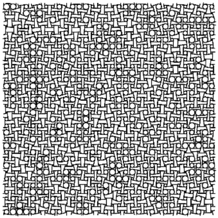

(b) $n_x = 16$

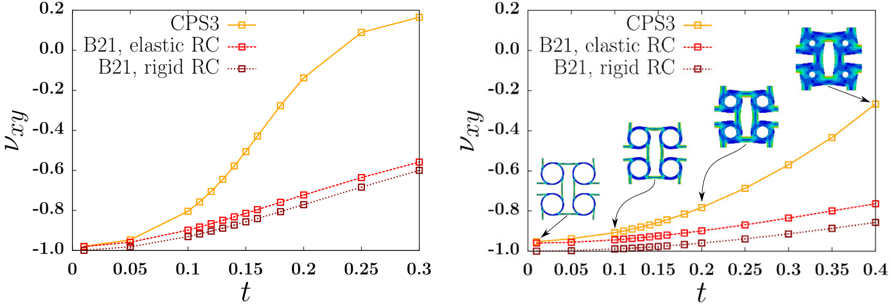

(a) $r = 0.15$ (b) $r = 0.40$

Figure: The influence of rib's thickness on the Poiison's ratio for 2 radii of RC: $r = 0.15$ (a) and $r = 0.4$ (b)

- CPS3 – planar elements,
- B21 elastic RC – Timoshenko beams with deformable RCs,
- B21 rigid RC – Timoshenko beams with rigid RCs,

Poisson's ratio as a function of the anisotropy

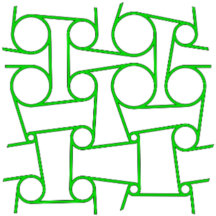

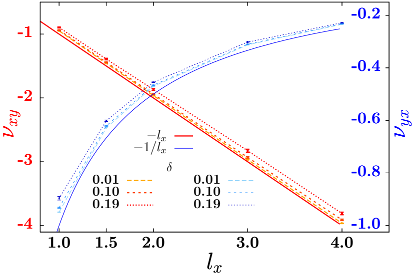

(a) $t = 0.05$

Poisson's ratio as a function of the anisotropy

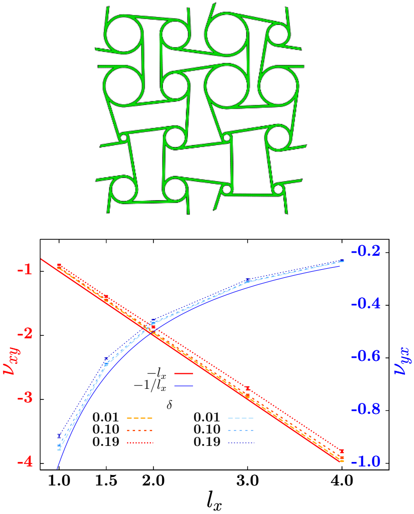

(a) $t = 0.05$

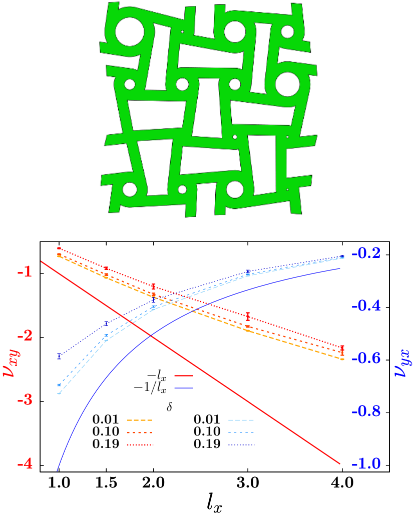

(b) $t = 0.2$

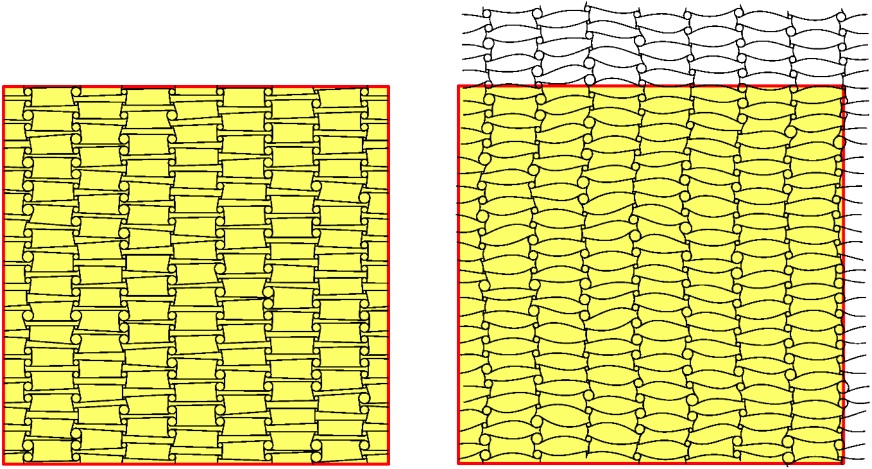

(a) Reference state

(b) Sample stretched along the X axis

Figure: $l_x = 4$, $\nu \approx -4 \ll -1$

Positional disorder – introduction

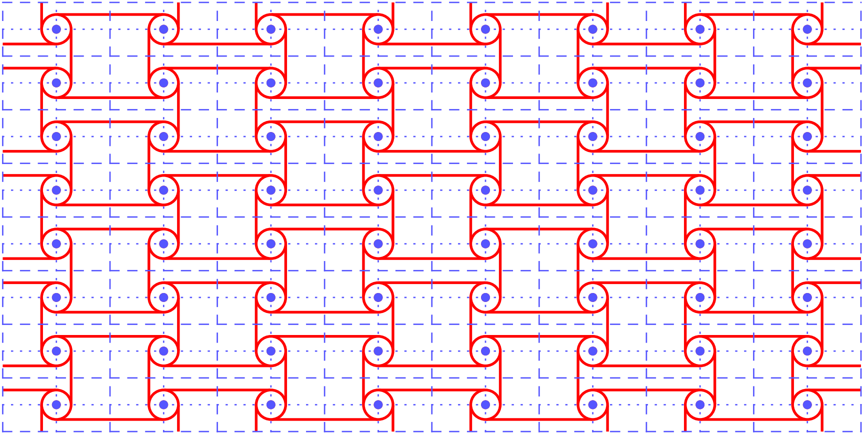

Positional disorder – introduction

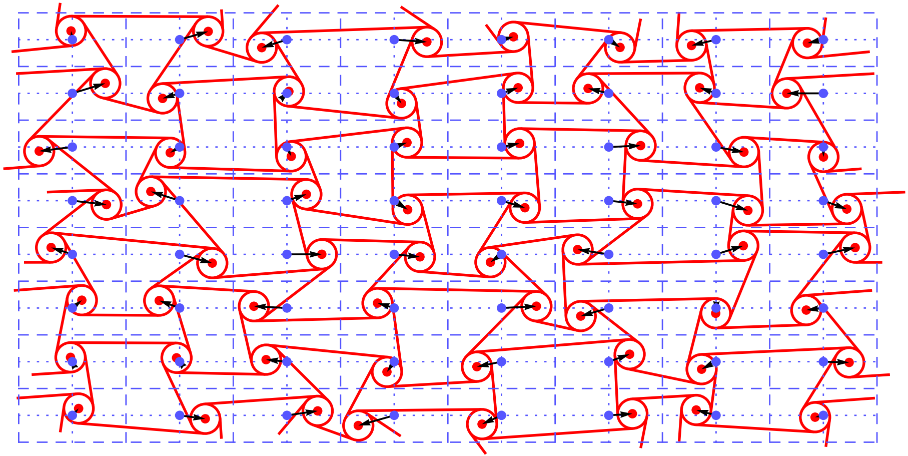

Positional disorder – introduction

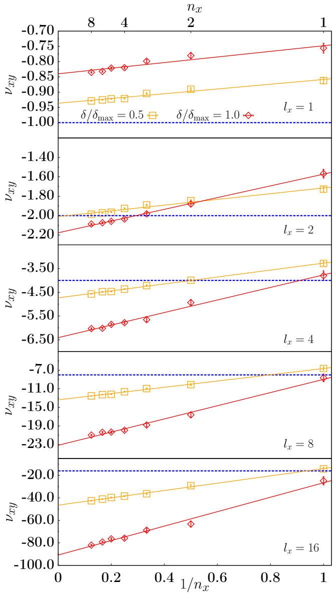

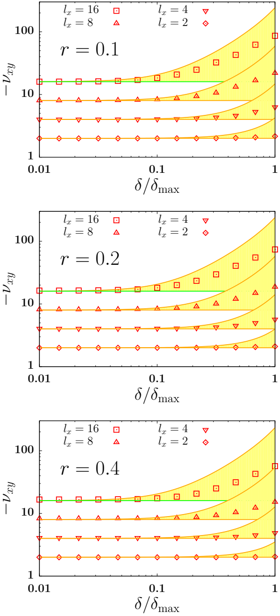

Technical issues

- Periodic mesh!
- Generation of the mesh when $l_x \gg 1$ in the case of planar elements(CPS3) requires an introduction of "artificial" cuts. This is time-consuming.

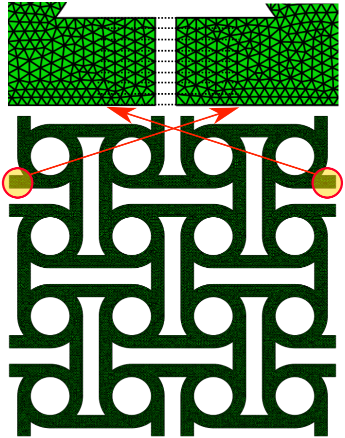

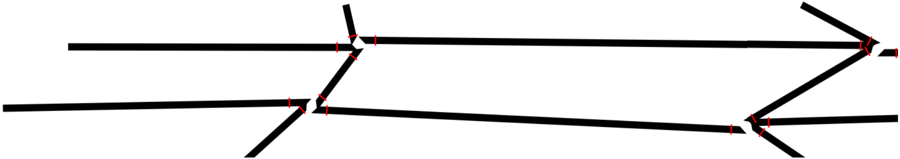

	l_x \ n_x	**1**	**2**	**4**	**8**	**16**
*.inp preparation time [min]	**1**	0.072	0.323	2.023	10.823	57.437
	4	0.092	0.453	2.862	15.578	87.122
	16	0.185	0.918	5.815	36.013	202.064
required memory [MB]	**1**	205	748	2 910	11 534	43 459
	4	432	1 627	6 372	25 272	97 078
	16	1 341	5 162	20 284	78 541	305 234
solving time [min]	**1**	0.163	0.638	3.506	15.099	68.114
	4	0.359	1.512	7.950	36.355	1 71.242
	16	1.568	6.368	28.250	118.200	501.749

CPS3

	l_x \ n_x	**1**	**2**	**4**	**8**	**16**
*.inp preparation time [min]	**1**	0.023	0.035	0.143	2.122	63.157
	4	0.027	0.037	0.148	2.160	63.257
	16	0.025	0.035	0.155	2.195	63.578
required memory [MB]	**1**	26	37	84	281	1 078
	4	30	54	157	581	2 283
	16	48	127	459	1 787	7 109
solving time [min]	**1**	0.005	0.011	0.036	0.181	0.770
	4	0.007	0.020	0.075	0.364	1.691
	16	0.016	0.059	0.230	1.300	5.809

B21

CPS3

	l_x \ n_x	**1**	**2**	**4**	**8**	**16**
*.inp preparation time [min]	**1**	0.072	0.323	2.023	10.823	57.437
	4	0.092	0.453	2.862	15.578	87.122
	16	0.185	0.918	5.815	36.013	202.064
required memory [MB]	**1**	205	748	2 910	11 534	43 459
	4	432	1 627	6 372	25 272	97 078
	16	1 341	5 162	20 284	78 541	305 234
solving time [min]	**1**	0.163	0.638	3.506	15.099	68.114
	4	0.359	1.512	7.950	36.355	1 71.242
	16	1.568	6.368	28.250	118.200	501.749

18

B21

	l_x \ n_x	**1**	**2**	**4**	**8**	[illegible]
*.inp preparation time [min]	**1**	0.023	0.035	0.143	2.122	63.1[illegible]
	4	0.027	0.037	0.148	2.160	63.257
	16	0.025	0.035	0.155	2.195	63.578
required memory [MB]	**1**	26	37	84	281	1 078
	4	30	54	157	581	2 283
	16	48	127	459	1 787	7 109
solving time [min]	**1**	0.005	0.011	0.036	0.181	0.770
	4	0.007	0.020	0.075	0.364	1.691
	16	0.016	0.059	0.230	1.300	5.809

	l_x \ n_x	**1**	**2**	**4**	**8**	**16**
*.inp preparation time [min]	**1**	0.072	0.323	2.023	10.823	57.437
	4	0.092	0.453	2.862	15.578	87.122
	16	0.185	0.918	5.815	36.013	202.064
required memory [MB]	**1**	205	748	2 910	11 534	43 459
	4	432	1 627	6 372	25 272	97 078
	16	1 341	5 162	20 284	78 541	305 234
solving time [min]	**1**	0.163	0.638	3.506	15.099	68.114
	4	0.359	1.512	7.950	36.355	1 71.242
	16	1.568	6.368	28.250	118.200	501.749

CPS3

40

	l_x \ n_x	**1**	**2**	**4**	**8**	[illegible]
*.inp preparation time [min]	**1**	0.023	0.035	0.143	2.122	63.1
	4	0.027	0.037	0.148	2.160	63.257
	16	0.025	0.035	0.155	2.195	63.578
required memory [MB]	**1**	26	37	84	281	1 078
	4	30	54	157	581	2 283
	16	48	127	459	1 787	7 109
solving time [min]	**1**	0.005	0.011	0.036	0.181	0.770
	4	0.007	0.020	0.075	0.364	1.691
	16	0.016	0.059	0.230	1.300	5.809

CPS3

	l_x \ n_x	**1**	**2**	**4**	**8**	**16**
*.inp preparation time [min]	**1**	0.072	0.323	2.023	10.823	57.437
	4	0.092	0.453	2.862	15.578	87.122
	16	0.185	0.918	5.815	36.013	202.064
required memory [MB]	**1**	205	748	2 910	11 534	43 459
	4	432	1 627	6 372	25 272	97 078
	16	1 341	5 162	20 284	78 541	305 234
solving time [min]	**1**	0.163	0.638	3.506	15.099	68.114
	4	0.359	1.512	7.950	36.355	1 71.242
	16	1.568	6.368	28.250	118.200	501.749

100

B21

	l_x \ n_x	**1**	**2**	**4**	**8**	[illegible]
*.inp preparation time [min]	**1**	0.023	0.035	0.143	2.122	[illegible]
	4	0.027	0.037	0.148	2.160	63.257
	16	0.025	0.035	0.155	2.195	63.578
required memory [MB]	**1**	26	37	84	281	1 078
	4	30	54	157	581	2 283
	16	48	127	459	1 787	7 109
solving time [min]	**1**	0.005	0.011	0.036	0.181	0.770
	4	0.007	0.020	0.075	0.364	1.691
	16	0.016	0.059	0.230	1.300	5.809

Conclusions

- Changing the anisotropy parameter (l_x) one can tune ν.
- **ν can reach any negative value.**
- For thin ribs the Timoshenko beam elements approximation gives satisfactory convergence.
- The disorder introduced by random RC radii has a negligible impact on ν.
- **Anti–chiral structures with rectangual symmetry are effective strain amplifiers with $\nu \ll -1$.**
- Thiner ribs give lower ν but the effective structure's stiffness is also decreased.

This work was supported by the (Polish) National Centre for Science under the grant NCN 2012/05/N/ST5/01476. Part of the simulations was performed at the Poznań Supercomputing and Networking Center (PCSS).

Special thanks to prof. K.W. Wojciechowski

Conclusions

- Changing the anisotropy parameter (l_x) one can tune ν.
- ν **can reach any negative value.**
- For thin ribs the Timoshenko beam elements approximation gives satisfactory convergence.
- The disorder introduced by random RC radii has a negligible impact on ν.
- **Anti–chiral structures with rectangual symmetry are effective strain amplifiers with $\nu \ll -1$.**
- Thiner ribs give lower ν but the effective structure's stiffness is also decreased.

This work was supported by the (Polish) National Centre for Science under the grant NCN 2012/05/N/ST5/01476. Part of the simulations was performed at the Poznań Supercomputing and Networking Center (PCSS).

Special thanks to prof. K.W. Wojciechowski

Conclusions

- Changing the anisotropy parameter (l_x) one can tune ν.
- ν **can reach any negative value.**
- For thin ribs the Timoshenko beam elements approximation gives satisfactory convergence.
- The disorder introduced by random RC radii has a negligible impact on ν.
- **Anti–chiral structures with rectangual symmetry are effective strain amplifiers with** $\nu \ll -1$**.**
- Thiner ribs give lower ν but the effective structure's stiffness is also decreased.

This work was supported by the (Polish) National Centre for Science under the grant NCN 2012/05/N/ST5/01476. Part of the simulations was performed at the Poznań Supercomputing and Networking Center (PCSS).

Special thanks to prof. K.W. Wojciechowski

Daily inspirations – melting snow is reentrant

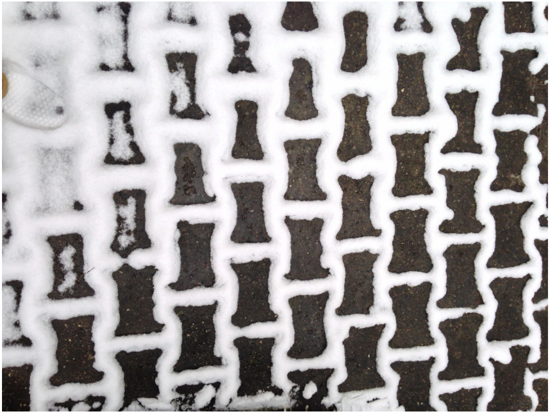

Daily inspirations – melting snow is reentrant

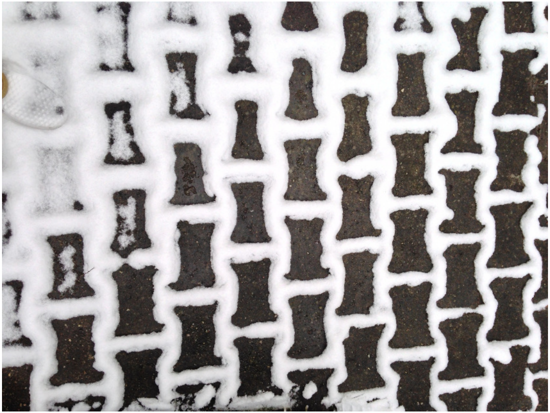

©Prof. K.W. Wojciechowski

Thank you